Influence of a Triblock Copolymer on Phase Behavior and Shear-Induced Topologies of a Surfactant Lamellar Phase

ARTICLE *in* LANGMUIR · MAY 2009

Impact Factor: 4.46 · DOI: 10.1021/la802943d · Source: PubMed

4 AUTHORS:

Shuji Fujii
Nagaoka University of Technology
36 PUBLICATIONS **199** CITATIONS
SEE PROFILE

Sven Koschoreck
RWTH Aachen University
5 PUBLICATIONS **80** CITATIONS
SEE PROFILE

Peter Lindner
Institut Laue-Langevin
152 PUBLICATIONS **4,413** CITATIONS
SEE PROFILE

Walter Richtering
RWTH Aachen University
237 PUBLICATIONS **6,067** CITATIONS
SEE PROFILE

Langmuir
Article
pubs.acs.org/Langmuir

Influence of a Triblock Copolymer on Phase Behavior and Shear-Induced Topologies of a Surfactant Lamellar Phase

S. Fujii,*[,†,‡] S. Koschoreck,[†] P. Lindner,[§] and W. Richtering*[,†]

[†]*Physical Chemistry, RWTH Aachen University, Landoltweg 2, 52070 Aachen, Germany* , [‡]*Department of Chemistry, Nagaoka University of Technology, 1603-1 Kamitomioka, Nagaoka, 940-2188, Japan* , *and* [§]*Institut Laue-Langevin, Grenoble, France*

Received September 8, 2008. Revised Manuscript Received March 30, 2009

The influence of a triblock copolymer, poly(ethylene oxide)$_{20}$-*b*-poly(propylene oxide)$_{70}$-*b*-poly(ethylene oxide)$_{20}$ (Pluronic P123) on the phase behavior and on the shear-induced multilamellar vesicle (MLV, also called Onion) formation in the lyotropic lamellar phase of the nonionic surfactant $C_{10}E_3$ was investigated by means of rheology, small-angle neutron scattering (SANS), and microscopy. Added triblock copolymer shifted the $L_\alpha-L_3$ phase transition to lower temperatures. In the presence of triblock copolymer, MLV structure was not stable and easily transformed back into the lamellar phase with increasing polymer concentration and temperature. In the study of the shear-induced MLV formation, we found an increase of the critical shear rate for the onset of the shear-thickening, which also indicates the instability of MLV in the presence of the triblock copolymer. No MLV formation was observed at high polymer concentration. Suppression of the shear-induced MLV formation might be attributed to the enhancement of the effective surface tension originating from the excluded volume effect between polymers adsorbed onto the membranes.

Introduction

A shear-induced formation of multilamellar vesicles (MLVs, also called "Onions") has been observed for many surfactant systems. Roux and co-workers found that the MLVs reveal long-time stability and a defined shear rate dependence of size,[1−3] which are interesting features for drug encapsulation in medical or cosmetic applications.[3−7] Although shear-induced MLV formation has attracted many researchers, only little is known about how a guest compound influences the thermodynamic properties of lamellae, especially for the MLV formation process.[8−10]

As a guest compound, triblock-copolymers composed of two blocks of poly(ethylene oxide) (PEO) and a poly(propylene oxide) (PPO) middle-block have been used to improve the steric stabilization of liposomes because of their biocompatibility.[11,12] The steric stabilization originates from the repulsive force according to the excluded volume effect between the hydrophilic PEO chains.[14−17] On the other hand, the PPO chains are more hydrophobic and can either adsorb onto the membrane or interpenetrate the membrane.[18−21] Therefore, there is a lot of interest to investigate how such polymers influence MLV formation and MLV stability.

Interactions of PEO chains grafted onto the lamellar membranes have been investigated by small-angle neutron scattering (SANS).[21,22,24−26] Important effects of the grafted-polymer chains are the modification of the physical properties of the lamellae, i.e., the elastic properties and the intermembrane interactions.[21,22,24−30,32,33] Grafted polymer chains significantly modify the spontaneous curvature c_0, the bending modulus κ, and the Gaussian modulus $\bar{\kappa}$ in order to compensate the polymer chain configuration entropy. Modification of the elastic properties of membranes causes a change in the morphology of membranes and its elasticity.[14,24−26,31−34] In addition to the elastic

*Corresponding author. E-mail: richtering@rwth-aachen.de; sfujii@mst.nagaokaut.ac.jp.

(1) Diat, O.; Roux, D.; Nallet, F. *J. Phys. IV* **1993**, *3*, 193–204.
(2) Diat, O.; Roux, D.; Nallet, F. *J. Phys. II* **1993**, *3*, 1427–1452.
(3) Diat, O.; Roux, D. *J. Phys. II* **1993**, *3*, 9–14.
(4) Roux, D.; Diat, O. French Patent number 92-04108, 1992.
(5) Freund, O.; Mahy, P.; Amedee, J.; Roux, D.; Laversanne, R. *J. Microencapsulation* **2000**, *17*, 157–168.
(6) Freund, O.; Amedee, J.; Roux, D.; Laversanne, R. *Life Sci.* **2000**, *67*, 411–419.
(7) Bernheim-Grosswasser, A.; Ugazio, S.; Gauffre, F.; Viratelle, O.; Mahy, P.; Roux, D. *J. Chem. Phys.* **2000**, *112*, 3424–3430.
(8) Schmidt, G.; Müller, S.; Schmidt, C.; Richtering, W. *Rheol. Acta* **1999**, *38*, 486–494.
(9) Berghausen, J.; Zipfel, J.; Lindner, P.; Richtering, W. *J. Phys. Chem. B* **2001**, *105*, 11081–11088.
(10) Yang, B.-S. R., Russel, W. B.; Prud'homme R. K. *Langmuir* 2005, *21*, 10038−10045.
(11) Woodle, M. C.; Matthay, K. K.; Newman, M. S.; Hidayat, J. E.; Collins, L. R.; Redemann, C.; Martin, F. J.; Papahadjopoulos, D. *Biochim. Biophys. Acta* **1992**, *1105*, 193–200.
(12) Woodle, M. C.; Newman, M. S.; Martin, F. J. *Int. J. Pharm.* **1992**, *88*, 327–334.
(13) Ligoure, C.; Bouglet, G.; Porte, G. *Phys. Rev. Lett.* **1993**, *71*, 3600–3603.
(14) Warriner, H. E.; Idziak, S. H. J.; Slack, N. L.; Davidson, P.; Safinya, C. R. *Science* **1996**, *271*, 969.
(15) Kostarelos, K.; Luckham, P. F.; Tadros, T. F. *J. Chem. Soc., Faraday Trans.* **1998**, *94*, 2159–2168.
(16) Johnsson, M.; Bergstrand, N.; Edwards, K.; Stalgren, J. J. R. *Langmuir* **2001**, *17*, 3902–3911.
(17) Silvander, M. *Prog. Colloid Polym. Sci.* **2002**, *120*, 35–40.
(18) Kostarelos, K.; Tadros, T. F.; Luckham, P. F. *Langmuir* **1999**, *15*, 369–376.
(19) Kostarelos, K.; Luckham, P. F.; Tadros, T. F. *J. Colloid Interface Sci.* **1997**, *191*, 341–348.
(20) Kostarelos, K.; Kipps, M.; Tadros, T. F.; Luckham, P. F. *Colloids Surf. A: Physicochem. Eng. Aspects* **1998**, *136*, 1–9.
(21) Masui, T.; Imai, M.; Nakaya, K.; Taniguchi, T. *J. Chem. Phys.* **2006**, *124*, 074904.
(22) Imai, M.; Mawatari, R.; Nakaya, K.; Komura, S. *Eur. Phys. J. E* **2004**, *13*, 391–400.
(23) Yang, B-S.; Lai, J.; Mihailescu, M.; Monkenbusch, M.; Richter, D.; Huang, J. S.; Kohn, J.; Russel, W. B.; Prudhomme, R. K. *Langmuir* **2002**, *18*, 6–13.
(24) Castro-Roman, F.; Porte, G.; Ligoure, C. *Phys. Rev. Lett.* **1999**, *82*, 109–112.
(25) Castro-Roman, F.; Ligoure, C. *Europhys. Lett.* **2001**, *53*, 483–489.
(26) Castro-Roman, F.; Porte, G.; Ligoure, C. *Langmuir* **2001**, *17*, 5045–5058.
(27) Helfrich, W. *Z. Naturforsch., Sect. A: J. Phys. Sci.* **1978**, *33*, 305–315.
(28) Leibler, S.; Lipowsky, R. *Phys. Rev. B* **1987**, *35*, 7004–7009.
(29) Helfrich, W. *J. Phys.: Condens. Matter* **1994**, *6*, A79–A92.
(30) Breidenich, M.; Netz, R. R.; Lipowsky, R. *Eur. Phys. J. E* **2001**, *5*, 403–414.
(31) Wennerstroem, H.; Daicic, J.; Olsson, U.; Jerke, G.; Schurtenberger, P *J. Mol. Liq.* **1997**, *72*, 15–30.
(32) Gommper, G.; Kroll, D. M. *Phys. Rev. Lett.* **1998**, *81*, 2284–2287.
(33) Golubovic, L.; Lubensky, T. C. *Phys. Rev. A* **1990**, *41*, 4343–4366.
(34) Morse, D. C. *Phys. Rev. E* **1994**, *50*, R2423–R2426.

properties, the modification of the intermembrane interaction, the compression modulus $\bar{B}$ also results in remarkable effects on the phase behavior. The compression modulus is mainly dominated by the entropic repulsive force between adjacent membranes, the so-called the Helfrich interaction.[27] Polymer chains grafted onto the membranes will enhance the repulsive force when the polymer size is large enough compared to the thickness of the water layer between bilayers.[13,24−26,28] Actually, the modification of these mechanical properties of the polymer-doped membranes was reported by some groups.[21−30] They have observed a strong increase in the bending modulus κ and a repulsive force between membranes. κ corresponds to the stiffness of a single lamellae and determines the amplitude of thermal undulations together with the compression modulus $\bar{B}$, corresponding to the strength of lamellar interactions. $\bar{\kappa}$ determines the lamellar connectivity. On the basis of free energy of bilayer systems, the morphology of membranes depends on the combination of two elastic moduli, κ and $\bar{\kappa}$. Stability of planar lamellae requires $2\kappa > -\bar{\kappa} > 0$. When $\bar{\kappa} > 0$, lamellae will be instable and transform into a sponge phase. When the spherical bending modulus $\tilde{\kappa}$, which can be expressed by the summation of two elastic moduli, is less than 0, $\tilde{\kappa} \equiv 2\kappa + \bar{\kappa} < 0$; on the other hand, spherical shells such as MLVs are favored. Thus, the modification of elastic properties and interlamellar interaction will strongly influence the nonequilibrium behavior of bilayer membrane systems under shear flow field, such as a shear-induced MLV formation.

Berghausen et al. and Yang et al. studied shear-induced MLV formation behavior for polymer-doped surfactant lamellar systems.[9,10] Berghausen et al. observed a suppression of shear-induced MLV in the presence of water-soluble polymers in ionic surfactant systems.[9] Contrary to that, Yang et al. observed a decrease in the critical shear rate and the MLV formation time for hydrophobically modified (poly(acrylic acid)) polymers anchored on the nonionic surfactant membrane.[10] These different effects of polymers on MLV formation motivated us to investigate how polymer chains grafted onto the membrane influence the dynamics. So far, little is known about the influence of a triblock copolymer on shear-induced MLV formation.

The aim in this study is to investigate how the PEO_{70}-*b*-PPO_{20}-*b*-PEO_{70} block copolymer (P123, BASF) influences the phase behavior and the pathway of the shear-induced MLV formation in the case of a well-known nonionic surfactant system composed of 40 wt % $C_{10}E_3$ in D_2O.[36−38,42,44−46] The observations will give further information about how grafted-polymer influences the shear-induced MLV formation process. The used polymer builds a planar bilayer at high concentrations, and MLV formation was found in ternary mixtures of P123, D_2O, and butanol.[35] Thus P123 is suited for investigating the influence of polymers on MLV formation and stability.[47,48]

Experimental Section

Materials and Sample Preparation. In this study, we used ternary mixtures of nonionic surfactant, $C_{10}E_3$, amphiphilic triblock copolymers, Pluronic P123, and D_2O. The nonionic surfactant $C_{10}E_3$ was purchased from Nikko Chemicals, Inc. The amphiphilic triblock copolymer (trade name Pluronic P123) was kindly supplied by BASF Corp. D_2O was purchased from Sigma Aldrich Chemicals Co. These chemicals were used without further purification. Nonionic triblock copolymer, Pluronics P123, is composed of two identical hydrophilic PEO tails and a hydrophobic PPO bounded between PEO tails. The degrees of polymerization of the PEO and PPO tails were 20 and 70, respectively. Thus Pluronic P123 has the following structure: PEO_{20}-*b*-PPO_{70}-*b*-PEO_{20}. In the sample preparation, the total concentration of compounds was fixed at 8 mM, which correspond to 40 wt % $C_{10}E_3$ in a D_2O binary system. The polymer-doped samples were prepared by replacing a certain mole fraction of 8 mM $C_{10}E_3$ with Pluronic P123, as expressed by following equation:

$$X_{P123} = \frac{n_{P123}}{n_{C10E3} + n_{P123}} \quad (1)$$

Here, n_{C10E3} and n_{P123} are the mole numbers of the $C_{10}E_3$ and P123, respectively. The mole fractions of P123 (polymer to surfactant mole ratio) were 0, 0.05, 0.1, 0.25, 0.5, and 2%. Composition and sample code are shown in Table 1. Samples were prepared by mixing these compounds and shaking them overnight. Thereafter they were equilibrated for a day. In this study, all viscosity measurements, microscopy observations, and rheo-SANS measurements were performed at 25 °C.

Phase Behavior. In order to study the phase behavior of P123-doped systems in the quiescent state, samples prepared were filled in test tubes and sealed carefully. The test tubes were placed in a water bath placed between polarizers in order to monitor the volume fractions of the strongly birefringent lamellar phase (L_α phase) and the isotropic sponge phase (L_3 phase). The water bath was temperature controlled with an accuracy of 0.1 °C. The temperature was increased stepwise and kept constant until phase equilibrium was reached, which took about 5 days, when the samples revealed a coexistence of both phases and more than 1 week for samples near the onset of phase separation.

Shear Experiments. Before starting a shear experiment, samples were presheared at $\dot{\gamma} = 10\ s^{-1}$ at 43 °C for sample #1,[36,38,41] 38 °C for sample #2, 37.5 °C for sample #3, and 33 °C for sample #5, respectively, in order to obtain prealigned lamellae with their surface normal to the velocity gradient (parallel orientation). After that, samples were cooled down to 25 °C without shearing. Thereafter the shear experiment was started.

Rheo-SANS measurements were performed at the D11 beamline at the Institute Laue-Langevin. The sample was sheared in a quartz Searl Cell (0.5 mm gap) by a stress controlled Bohlin Rheometer (CVO-120). The two-dimensional (2D) scattering pattern shows sharp Bragg peaks originating from the repeating distance between lamellar membranes with its long-range positional order. Measurements in this study were performed in the radial beam configuration, in which the neutron beam passes the sample along the velocity gradient direction and allows monitoring intensity changes in the flow and neutral direction. In order to study the dynamic phase diagram of the systems under shear, Rheo-SANS measurements were performed with a constant heating rate of 0.17 K/min at a shear rate of $10\ s^{-1}$. Time-resolved rheo-SANS measurements were carried out in a q-range of 0.02−0.13 $Å^{-1}$, which is wide enough to detect the Bragg peak from the lamellar systems of the $C_{10}E_3$ system with a wavelength of 0.45 nm.[36] Acquisition time in the time-resolved experiments was 50 s.

Viscosity measurements were performed using a CVO-120 from Bohlin Co., Ltd., equipped with a Mooney Cell with both the strain and stress control modes. Gap size between the inner and outer cell was 1 mm, which is large enough to avoid the gap size effect on the MLV size and viscoelasticity for the $C_{10}E_3/D_2O$ binary system.[42]

Microscopy experiments under shear were performed by means of a Linkam shear cell, CSS 450, which has a plate−plate shear geometry, attached onto a Leica microscope (DMLB) between crossed polarizers. The images were obtained in the middle of the gap to avoid wall effects. The gap size between the upper and

(35) Zipfel, J.; Lindner, P.; Tsianou, M.; Alexandridis, P.; Richtering, W. *Langmuir* **1999**, *15*, 2599–2602.
(36) Nettesheim, F.; Zipfel, J.; Olsson, U.; Renth, F.; Lindner, P.; Richtering, W. *Langmuir* **2003**, *19*, 3603–3618.
(37) Le, T. D.; Olsson, U.; Mortensen, K.; Zipfel, J.; Richtering, W. *Langmuir* **2001**, *17*, 999–1008.
(38) Le, T. D.; Olsson, U.; Mortensen, K. *Physica B* **2000**, *276*, 379–380.

Table 1. Sample Code and Composition of P123-Doped Lamellae Samples

sample code	#1	#2	#3	#4	#5	#6
P123/mol%	0	0.05	0.1	0.25	0.5	2.0

lower plates was fixed at 500 μm, which is sufficiently large to avoid gap size effects for the $C_{10}E_3/D_2O$ binary system.[42]

Results and Discussion

Influence of P123 on the Phase Behavior at the Quiescent State. The mole fractions of P123, X_{P123}, were 0, 0.05, 0.1, 0.25, 0.5, and 2%. The radius of gyration of PEO in water was roughly estimated as R_G = 0.64 nm by employing the experimentally determined relationship, $R_G/\text{nm} = 0.1078 M_{PEO}^{0.635}$.[43] One expects two kinds of polymer structures on the membranes depending on the polymer-to-surfactant mole ratio X_{P123}: a mushroom-like structure of PEO tails at low X_{P123} and a brush-like structure at high X_{P123}. The crossover between them was roughly estimated to be $X^*_{P123} \approx 3.7\%$ by considering the overlap limit of PEO chains on the plane membranes. Thus, in all of the systems, the polymer structure is considered to be mushroom-like. The thickness of the water layer in the $C_{10}E_3/H_2O$ system is 3.6 nm, which is larger than twice the diameter of the PEO chain. Therefore the PEO chain has enough space in the water layer, and no configuration entropy loss of polymer chain is expected. Entropy loss of polymer chains will drive the lamellae−lamellae phase separation because of the depletion interaction. Actually, we have not observed any signal of the appearance of the lamellae−lamellae phase separation in SANS.[21,23,26]

Figure 1 shows the temperature dependence of the volume fractions of the lamellar phase (L_α phase) and sponge phase (L_3 phase) in the quiescent state. The system shows a phase separation into $L_\alpha - L_3$ coexistence region with increasing temperature. Upon further increase of the temperature, the L_3 phase appears after the coexistence region. Increasing the polymer content remarkably reduces the phase transition temperature from L_α to $L_\alpha - L_3$ coexistence to L_3, indicating that P123 adsorbed onto the membranes favors a highly connected sponge phase rather than planar lamellae.

Isothermal SANS measurements were performed in order to investigate the polymer influence on the lamellar order in the quiescent state. Figure 2 shows SANS profiles for samples with different polymer mole fractions at 25 °C. SANS patterns display the correlation peak at a constant **q** vector. The constant peak position confirms that the polymer is well miscible in the surfactant lamellar phase and has no significant influence on the lamellar repeat distance. No significant polymer−polymer interactions that could cause a lamellar−lamellar phase separation are observed.

Dynamic Phase Behavior under Shear. Figure 3 shows the temperature dependence of rheo-SANS patterns obtained with radial beam configuration at a shear rate of 10 s^{-1}. Temperature was scanned from low to high temperature with a constant heating rate of 0.17K/min. In Figure 3a, characteristic 2D-SANS patterns observed for typical membrane topologies for a $C_{10}E_3/D_2O$ binary system are shown in order to compare with the polymer-doped systems. Five domains in Figure 3a correspond to MLVs (domain I), multilamellar cylinders (MLCs) or coherently undulating lamellar membranes (domain II), mainly parallel oriented lamellae coexisting with a small amount of perpendicular oriented lamellae (domain III), a coexistence phase of a lamellar structure with a perpendicular orientation and a sponge phase (domain IV), and a sponge phase at high temperatures (domain

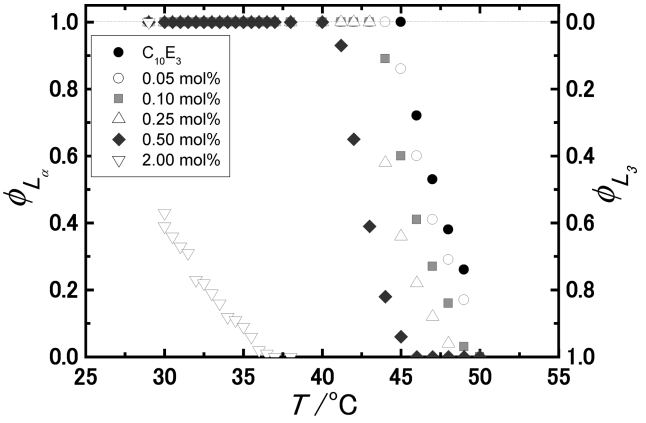

Figure 1. Volume fraction of the lamellar phase (L_α phase) and the sponge phase (L_3 phase) as a function of temperature for samples with different P123 mole fractions.

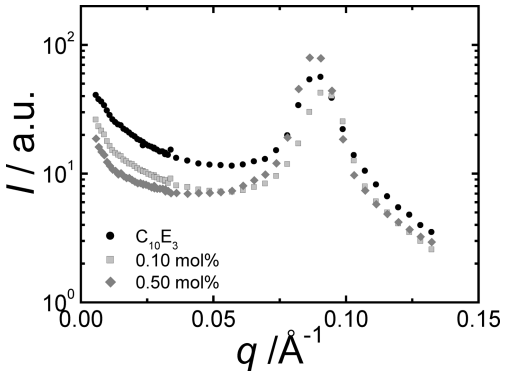

Figure 2. Representative SANS spectra of the lamellar phase for a $C_{10}E_3/D_2O$ binary system and two polymer-doped ternary systems at 25 °C. The polymer-to-surfactant mole fraction was 0, 0.1, and 0.5 mol %.

V), respectively. A detailed discussion of the pure $C_{10}E_3$/water system was given by Nettesheim et al. and Le et al.[36−38] In short, MLVs (domain I) show an isotropic Bragg peak pattern. For MLCs or coherent undulating lamellae (domain II), I_n, the intensity at the peak in the neutral direction, develops and reaches a maximum, whereas I_f, the intensity at the peak in the flow direction, decreases and approaches a minimum. The asymmetric intensity distribution is quite characteristic for this topology.[35,36] For the parallel-oriented lamellae with their surface normal to the gradient direction, the so-called parallel or *C*-orientation (domain III), I_n decreases and reaches a constant intensity. In the L_α- and L_3-phase coexisting region (domain IV), a correlation peak from the L_3 phase superimposing the Bragg peak from the L_α phase can be seen. In domain V, only the isotropic correlation peak is visible.

Typical 2D-SANS patterns under shear at 10 s^{-1} at several temperatures for the polymer-doped systems are shown in Figure 3b. The evolution of the L_α correlation peak intensities in the neutral (I_n) and flow (I_f) directions with temperature is summarized in Figure 4. 2D-SANS patterns and their temperature development shown in Figure 3b and 4 show qualitatively similar behavior to that of the binary $C_{10}E_3/D_2O$ system.[36] However, the phase boundaries between different topologies remarkably depend on the polymer content. The results are summarized in Figure 5 as a dynamic phase diagram. We should mention that the results shown in Figures 3, 4, and 5 do not exactly correspond to the steady state under shear because the structural transformation takes a long time compared to the heating rate of 0.17 K/min. Therefore, these figures might not be

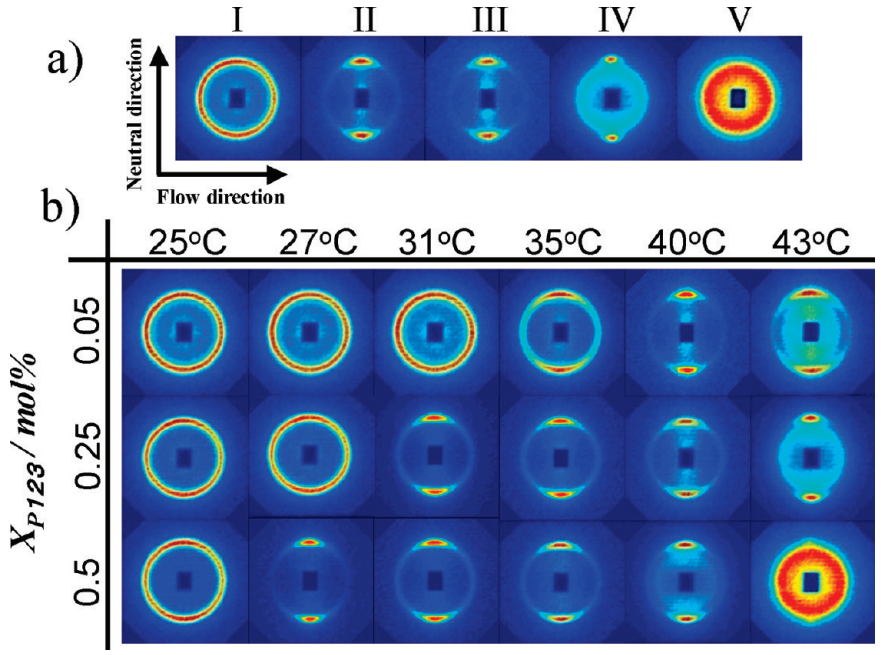

Figure 3. Temperature and P123 mol fraction dependence of rheo-SANS profiles in the flow-neutral plane at a shear rate of 10 s^{-1}. (a) Typical 2D-SANS patterns observed with characteristic phases for the $C_{10}E_3/D_2O$ binary system. Each SANS profile corresponds to a different membrane topology. (I) MLVs at 25 °C; (II) MLCs or coherently undulating bilayers at 36.5 °C; (III) L_α at 39.1 °C; (IV) $L_\alpha + L_3$ at 44.2 °C; and (V) L_3 at 43 °C. (b) Rheo-SANS profiles as a function of the polymer mole fraction and temperature for the polymer-doped $C_{10}E_3$ systems at a shear rate of 10 s^{-1}.

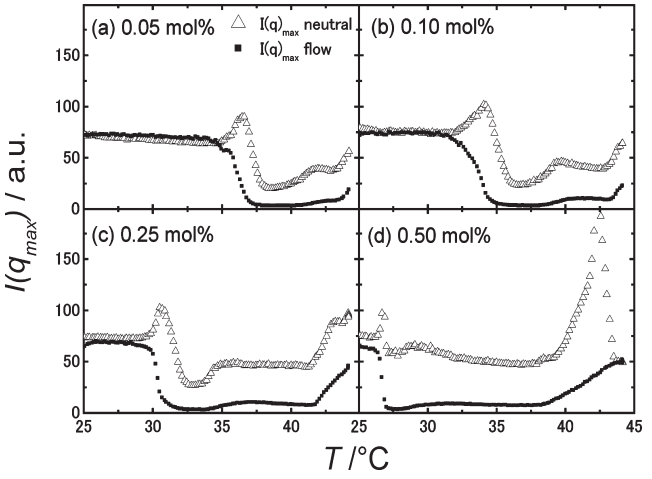

Figure 4. Temperature dependence of the Bragg peak intensities in the neutral and flow directions for the polymer-doped $C_{10}E_3$ systems at a shear rate of 10 s^{-1}.

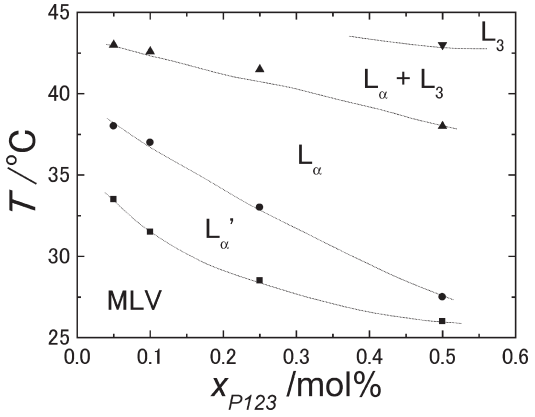

Figure 5. Dynamic phase diagram for the polymer-doped $C_{10}E_3$ ternary systems under a shear of 10 s^{-1}.

compared directly with the phase diagram at equilibrium state in Figure 1. However, the shear rate should act as a "pre-shear" in the successive increase in the temperature. Thus, the data in Figures 3, 4, and 5 might be not far from the equilibrium state. At least, the heating rate does not influence the qualitative behavior.

Increasing the polymer content lowers the transition temperatures. Especially, MLVs (domain I) and L_α's (domain II) are remarkably suppressed by increasing the polymer content. In contrast, the L_α phase becomes a stable structure as a steady state under shear, which indicates that the membranes are stiffened by adding the polymer. Stiffening of the membranes by adding Pluronic has been observed for similar surfactant systems ($C_{12}E_5$/pluronic/water ternary systems).[21] Thus, it is plausible to consider in this study that the polymer chains adsorbed onto the membrane enhance the bending modulus. Stiffening of the membranes will result in the hindrance of shear-induced MLV formation. Additionally, an increase in the effective thickness of the membranes due to the adsorbing polymer has also been reported.[21,26] The results in this study also indicate that the adsorbed polymer chains modify the mechanical properties of a membrane.

Shear-Induced MLV Formation. The influence of P123 on shear-induced MLV formation at constant temperature was investigated by viscometry and rheo-SANS measurements at four different polymer contents. In Figure 6, the time dependence of the transient viscosity and the Bragg peak intensities in the neutral and flow directions at the shear rate of 10 s^{-1} are compared as a function of shear strain.

$C_{10}E_3$ without Polymer. In previous studies for $C_{10}E_3/D_2O$, the MLV formation process was classified into two steps that could be deduced from rheo-SANS profiles.[36] Before shearing, low values of I_f and I_n indicate a parallel orientation of the lamellae. When the shear flow is applied, I_n starts increasing significantly and reaches a maximum. The strong increase in I_n indicates that a certain amount of the lamellar membranes orient with their surface normal into the neutral direction.

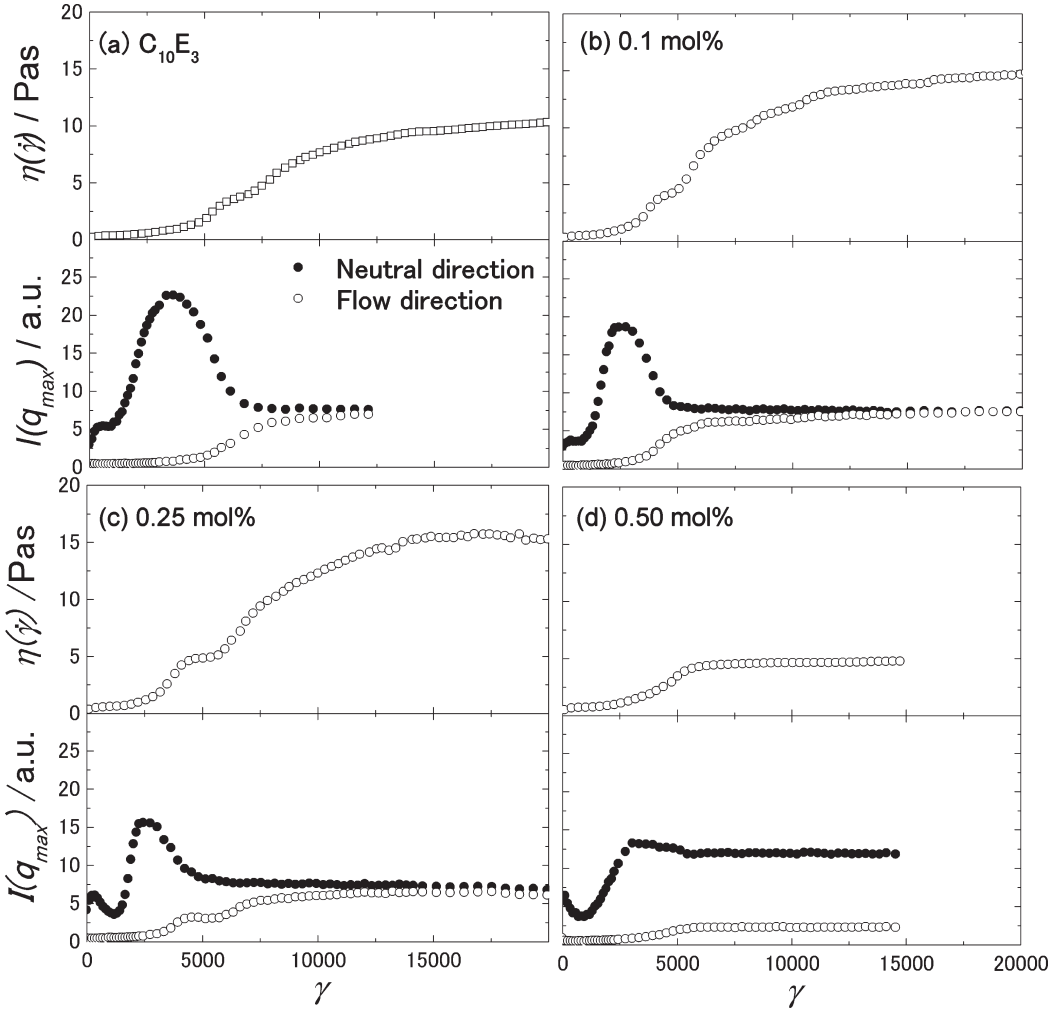

Figure 6. Time evolution of the transient viscosity and Bragg peak intensities in the neutral and flow directions for the $C_{10}E_3/D_2O$ binary system and polymer-doped $C_{10}E_3$ ternary systems with different mole fractions of P123. Here the shear rate was fixed at a shear rate of 10 s^{-1}.

The appearance of the intensity maximum in the first step is a characteristic indication of the MLC structure or coherently undulating membrane formation. This structure as an intermediate state might be similar to that in domain II observed in the temperature sweep in Figure 4. At this stage, the transient viscosity does not show a remarkable increase. In the second step, I_n starts to decrease, whereas I_f starts to increase simultaneously. I_n and I_f change continuously and level off. At the same time, the transient viscosity starts to increase until a "shoulder" is observed, which marks the structural transformation from MLC or coherent undulation into a new adjusted structure. The increase in I_f indicates the appearance of lamellae oriented with their surface normal into the flow direction, so-called transverse orientation or b-orientation. Thus, the new adjusting structure would be attributed to the buckled membranes or isotropic orientation of lamellae, i.e., MLVs. The shoulder in the transient viscosity would be a signal for the MLC-to-MLV transformation. Then I_f and I_n approach one another corresponding to a transition from buckled membrane or polydispersed MLVs into monodispersed MLV structure. The transient viscosity increases further and levels off when steady state is reached.

Polymer-Doped Systems. Polymer-doped systems also show an MLV formation process qualitatively similar to the pure surfactant system, except for the system with high polymer content, X_{P123} = 0.5 mol %. At low mole fraction of polymer with 0.1 and 0.25 mol % (Figure 6b,c), the appearance of the characteristic shoulder in the viscosity curves and the maximum intensity in I_n reduce to small strain region. Also, the shoulder as an intermediate state in the transient viscosity appears to be clear. The addition of a small amount of polymer seems to promote the MLC or coherently undulating membrane formation and initialization of the MLV formation compared to the pure surfactant system. However, the maximum intensity of I_n is decreased with increase in the polymer content. MLC or buckling lamellae should show a pronounced maximum intensity of I_n, as seen for the pure surfactant system. There would be less curved membranes at intermediate state and thus imperfect MLC or coherently undulation. It should be noted that the transient behavior of I_f at 0.25 mol % also shows a shoulder at the same time as the development of shoulder in the viscosity. The appearance of the shoulder in I_f corresponding to that of the viscosity clearly indicates a two-step evolution of the shear-induced MLV formation. It is noticeable that the viscosity at the shoulder is almost similar for all samples. At 0.5 mol% of P123 (Figure 6d), the viscosity does not change but stays at a value comparable to that of the shoulder for other samples. I_n and I_f do not show any signal for the MLC formation, i.e., the shoulder. At 0.5 mol %, only planar lamellar exists. Thus it seems that the membranes are stiffened in the presence of polymers. The observation indicates that there are two processes for the shear-induced L_α-to-MLV transformation: (i) shear-induced MLC formation or coherently undulation and (ii) MLC or coherently undulation to MLV

formation. Two processes might be controlled by different mechanisms and parameters. Suppression of MLV formation as signaled by the shoulder in Figure 6 indicates that the stiffness of membrane especially influences the second step, i.e., the structural development from imperfect MLC or coherently undulation to MLVs.

Figure 7 shows the steady state viscosity as a function of the shear rate for the polymer-doped systems. We observed shear-thickening and shear-thinning for the pure surfactant system. It is known that the shear-induced MLV formation for the nonionic surfactant systems is accompanied with shear-thickening.[36,41] In the polymer-doped system with 0.25 and 0.50 mol % of polymer concentration, Newtonian behavior at low shear rates are observed. The initialization of the shear thickening would be regarded as the onset of the MLV formation. In this diagram, a critical shear rate for the shear-thickening behavior was broadly defined as a boundary where the viscosity stays in the Newtonian region. The critical shear rate as a measure for the onset of shear-thickening shifts to higher shear rates in the presence of P123, even though the MLV formation time is shortened at low polymer contents (Figure 6). Thus, the MLV formation for the polymer-doped system needs more mechanical energy as compared to the $C_{10}E_3/D_2O$ system, but the MLV formation is easily achieved once the critical shear rate is exceeded. Here we should mention that the viscosity in Figure 7 does not fit to the steady state viscosity shown in Figure 6. The difference might be caused by the different gap size.[42] However, the qualitative behavior of the time-resolved measurement in Figure 6 is not influenced. It should be mentioned that the steady state viscosity in the high shear rate regions could not be achieved because of a strong Weissenberg effect of polymer-doped systems.

Shear Rate Dependence of the MLV Size. Figure 8 presents microscopy images and corresponding fast Fourier transform (FFT) images at three different shear rates for the pure surfactant system (a) and the polymer-doped sample composed of 0.1 mol % P_{123} (b), respectively. At 0.3 s^{-1}, corresponding to the low shear rate part in the shear-thickening region for both systems (Figure 7), bright birefringence originating from defects instead of MLVs can be seen for both systems. Densely packed monodisperse MLVs appear for the pure surfactant system at 7 s^{-1}. The FFT image shows sharp Bragg peaks, indicating that the diffraction pattern corresponds to a monodisperse MLV structure. For the polymer-doped sample, MLVs have also been seen in the microscopic image. The Bragg peaks from FFT images of the polymer-doped samples are further from the center than that of pure surfactant MLV. Thus, MLVs of polymer-doped samples are smaller than those of the pure surfactant system. However, this result seems to contradict the increase in the stiffness of membranes. An increase of the rigidity of membrane should induce large size of the MLVs. The diffuse Bragg peak in the FFT image indicates that the MLVs are not packed well but are rather disordered in the presence of polymer. At 10 s^{-1}, corresponding to the shear-thinning region, the polymer-doped sample also shows well-packed MLV structure as well as for the pure surfactant system. The smaller MLV size of the polymer-doped ternary systems in comparison with the $C_{10}E_3/D_2O$ binary system may be caused by a polymer chain distribution on the membrane during the MLV formation process. Shear-induced MLVs are densely packed with polygonal shape. At the side of the polygon, membranes suffer significant bending. If the segregation of polymer chains on the membrane is allowed, the polymer chain may concentrate on the side of the polygon and compensate for the elastic energy required to bend membranes, because the polymer chain has a high curvature. Smaller MLVs as compared to the pure surfactant system may be formed.

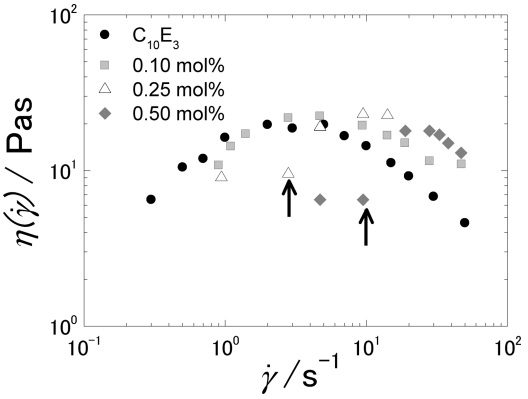

Figure 7. Shear rate dependence of the steady state viscosity for $C_{10}E_3/D_2O$ binary system and the polymer-doped $C_{10}E_3$ ternary systems. Arrows show the boundary between the Newtonian and the shear-thickening regions.

Figure 9 shows a shear rate dependence of the MLV radius estimated by microscopy observations. Evolution of the MLV size with shear rate not only for the pure surfactant but also for polymer-doped systems is described by a power law relation with an exponent of −0.5. van der Linden suggested that MLV size is determined by the mechanical balance between an effective surface tension of MLV and the applied shear stress by[39,40]

$$R_{\mathrm{MLV}} \approx \frac{\tau_{\mathrm{eff}}}{\sigma} \qquad (2)$$

Here, τ_{eff} is the effective surface tension described as $\tau_{\mathrm{eff}} \approx (\kappa \bar{B})^{1/2}$ and σ is applied shear stress. The average MLV radius was plotted as a function of the inverse of the shear stress in Figure 10. In our previous study, eq 2 holds only for the shear-thinning region but fails in the shear-thickening region.[42] In Figure 10, all of the data in both of the shear-thickening and shear-thinning regions are shown. Filled and open symbols correspond to the shear-thinning and shear-thickening regions, respectively. All data in the shear-thinning region could be fitted with eq 2 in spite of the presence of polymer. However, the data in the shear-thickening region deviate from the linear relation as shown in previous work. We have roughly estimated the slope in the shear-thinning region to be $\tau_{\mathrm{eff}} \equiv 3.67 \pm 0.52 \times 10^{-4}$. However, the estimated surface tension includes ±15% of variation. Because of the difficulty in measuring the steady state viscosity of the polymer-doped systems, we could not take enough data points to estimate the effective surface tension for each system. However, polymer content dependence of the effective surface tension would be included in the ±15% of variation. The effective surface tension is given by the product of κ and $\bar{B}$ as shown in eq 2. The influence of grafted-polymer chains on κ and $\bar{B}$ was studied by different groups.[21,24−26] They have observed the increase in the product $\kappa\bar{B}$. Masui et al. found that the excluded volume effect between the grafted-polymer chains (PEO chains) causes an effective lateral pressure and increases the

(39) van der Linden, E.; Hogervorst, W. T.; Lekkerkerker, H. N. W. *Langmuir* **1996**, *12*, 3127–3130.
(40) van der Linden, E.; Droege, J. H. M. *Physica A* **1993**, *193*, 439–447.
(41) Oliviero, C.; Coppola, L.; Gianferri, R.; Nicotera, I.; Olsson, U. *Colloids Surf., A* **2003**, *228*, 85.
(42) Fujii, S.; Richtering, W. *Eur. Phys. J. E* **2006**, *19*, 139–148.
(43) Cabane, B.; Duplessix, R. *J. Phys. (Paris)* **1993**, *51*, 1313.
(44) Medronho, B.; Fujii, S.; Richtering, W.; Miguel, M. G.; Olsson, U. *Colloid Polym. Sci.* **2005**, *284*, 317–321.
(45) Medronho, B.; Shafaei, S.; Szopko, R.; Miguel, M. G.; Olsson, U.; Schmidt, C. *Langmuir* **2008**, *24*(13), 6480–6486.
(46) Koschoreck, S.; Fujii, S.; Lindner, P.; Richtering, W. *Rheol. Acta* **2009**, *82*, 231–240.
(47) Holmqvist, P.; Alexandridis, P.; Lindman, B. *J. Phys. Chem. B* **1998**, *102*, 1149–1158.

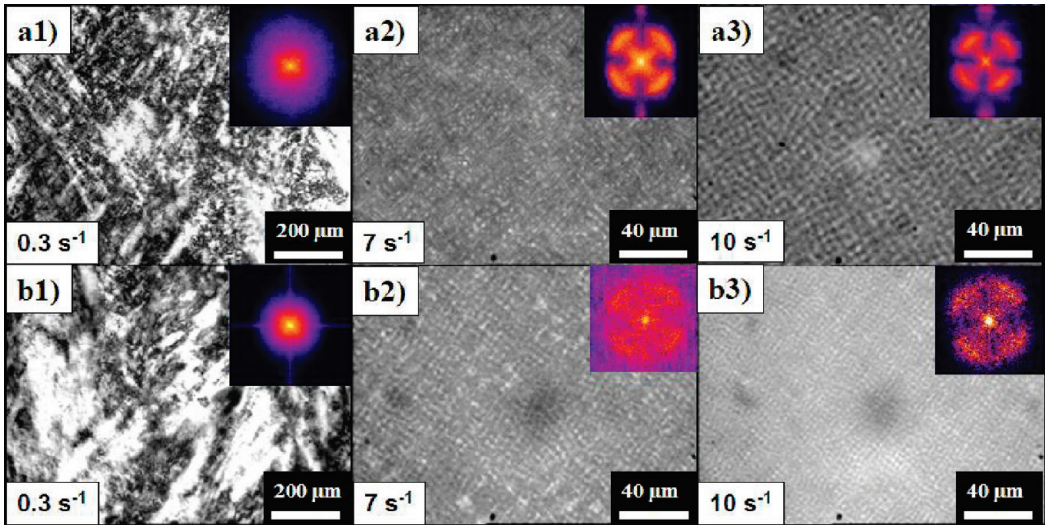

Figure 8. Microscopy images and FFT images for (a) the $C_{10}E_3/D_2O$ binary system and (b) the polymer-doped $C_{10}E_3$ system with X_{P123} = 0.1 mol % under shear.

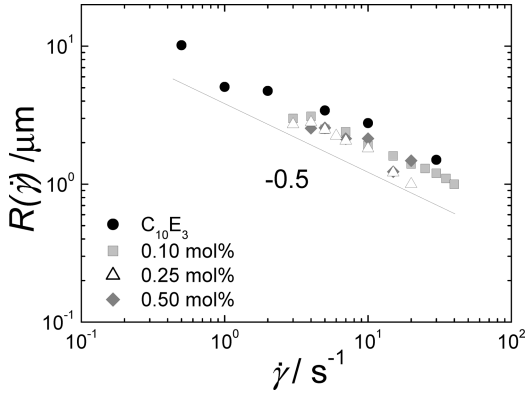

Figure 9. MLV radius as a function of the shear rate for the $C_{10}E_3/D_2O$ binary system and polymer-doped $C_{10}E_3$ ternary system with X_{P123} = 0.1, 0.25, and 0.5 mol %.

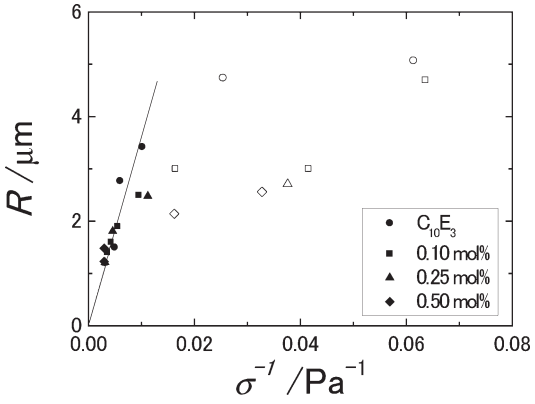

Figure 10. MLV radius as a function of the reciprocal shear stress calculated by producing the applied shear rate and steady state viscosity. Slope of the solid line shows the effective interfacial tension estimated to be $3.67 \pm 0.52 \times 10^{-4}$ Nm^{1-} by eq 2. Filled and open symbols belong to the shear-thinning and shear-thickening regions, respectively.

effective bending modulus κ_{eff} of polymer-decorated membranes in $C_{12}E_5$/pluronic/water ternary systems.[21] Castro-Roman et al. found that the increase in the membrane thickness also enhances the compression modulus in addition to the modification of the bending modulus for the polymer-doped lamellar phases.[24−26] An increase in $\kappa\bar{B}$ will remarkably suppress the strength of interlamellar fluctuations and result in prevention of the MLV formation.[27,39,40] Therefore, suppression of the shear-induced MLV formation observed in this study might be attributed to the enhancement of the effective surface tension, $\kappa\bar{B}$.

In the Zilman and Granek theory, the coupling between the shear flow and short wavelength undulation yields the buckling of membranes, which results in the MLV formation.[49] An increase in the effective surface tension originating from the excluded volume effect between polymers and from the increase in the membrane thickness will smooth out the membranes. Thus, the wavelength of membrane undulation would be increased and easily deformed by shear. Promoted MLV formation process under shear shown in Figure 6b,c might be also attributed to the enhancement of $\kappa\bar{B}$. The critical shear rate for the buckling instability needed to form MLV structure is also given as a function of the effective surface tension of the membrane in the Zilman and Granek theory. Their prediction seems to qualitatively correspond to the observation of the increase in the critical shear rate for the shear-thickening viscosity in Figure 7.

Conclusions

The influence of the triblock copolymer PEO_{20}-*b*-PPO_{70}-*b*-PEO_{20} (Pluronic P123, BASF) on phase behavior and shear-induced MLV formation was studied for a nonionic lamellar phase composed of 40 wt % $C_{10}E_3$ in water.

Both the equilibrium phase behavior and the dynamic phase behavior under shear showed that the addition of triblock copolymer significantly reduces the $L_\alpha-L_3$ phase boundary with increasing polymer concentration, and polymer-doped membranes favor planar L_α phase as compared to MLV under shear.

The shear-induced MLV formation is effectively influenced by adding polymers. Addition of polymer shortens the initialization of structural development from L_α to imperfect MLC or coherently buckled membranes. However, further structural development from MLC or coherent undulation into the MLV is significantly suppressed. The results obtained in this study

(48) Zipfel, J.; Berghausen, J.; Schmidt, G.; Lindner, P.; Alexandridis, P.; Richtering, W. *Macromolecules* **2002**, *35*, 4064–4074.

(49) Zilman, A. G.; Granek, Z. *Eur. Phys. J. B* **1999**, *11*, 593–608.

indicate that there are two processes for the shear-induced L_α-to-MLV transformation: the first is shear-induced MLC or coherently undulation formation, and the second is the MLV formation. The shift of the critical shear rate of the onset of shear-thickening and the suppression of the shear-induced MLV formation would be attributed to the increase in the effective surface tension of the membranes caused by the excluded volume effect between hydrophilic PEO parts of the polymer chain grafted onto the membranes.

Acknowledgment. Financial support by the Deutsche Forschungsgemeinschaft is gratefully acknowledged.